



Published in final edited form as:

*Cancer Res.* 2010 May 15; 70(10): 3965–3974. doi:10.1158/0008-5472.CAN-09-3450.

## Deregulated estrogen receptor alpha and p53 heterozygosity collaborate in the development of mammary hyperplasia

Edgar S. Díaz-Cruz<sup>1</sup> and Priscilla A. Furth<sup>1,2</sup>

<sup>1</sup>Department of Oncology, Lombardi Comprehensive Cancer Center, Georgetown University, Washington, DC, 20057

<sup>2</sup>Department of Medicine, Lombardi Comprehensive Cancer Center, Georgetown University, Washington, DC, 20057

### Abstract

Both increased Estrogen Receptor (ER) $\alpha$  expression and germline disruption of one p53 allele increase breast cancer risk in women. Genetically engineered mouse models of deregulated ER $\alpha$  expression and p53 haploinsufficiency were used to investigate similarities and differences of each genetic lesion alone and in combination on mammary preneoplasia development. Each genetic lesion independently and in combination led to development of age-dependent preneoplasia but the highest prevalence was found in compound mice with increased ER $\alpha$  expression coupled with p53 heterozygosity. All genetic lesions were associated with ERK1/2 activation, however, only p53 heterozygous and compound mice showed increased levels of phosphorylated AKT and decreased p27 expression. The highest levels of cell proliferation were found in compound mice, but increased levels were also found with either increased ER $\alpha$  expression or p53 heterozygosity. Mice with increased ER $\alpha$  expression showed predicted higher levels of nuclear localized ER $\alpha$ , but this was attenuated in compound mice in association with a relative increase in Src phosphorylation. Parity protection was limited to p53 heterozygous mice and not found in mice with increased ER $\alpha$  alone. In summary, increased and deregulated ER $\alpha$  collaborates with p53 heterozygosity in increasing the risk of mammary preneoplasia development.

### Keywords

p53; estrogen receptor; mammary hyperplasia; parity; transgenic mouse model

### Introduction

Breast cancer is the second leading cause of cancer death in women with prevalence increasing with age (1). Breast cancer develops as molecular changes accumulate in the ductal epithelium giving rise to precursor lesions such as atypical ductal hyperplasias, which may progress to ductal carcinoma *in situ* (DCIS) and invasive breast cancer (2). Breast cancer is associated with somatic genetic and epigenetic alterations in the breast tissue such as tumor suppressor gene mutation or other molecular changes that compromise their function.

The tumor suppressor p53 plays a role in mediating cell response to various stresses by inducing or repressing genes involved in cell cycle arrest, senescence, apoptosis, DNA repair, and angiogenesis (3). Alterations to p53 are commonly detected in primary human breast tumors (4), reported in 30-40% of human breast cancers (5) and about 25% of all preinvasive DCIS

---

To whom correspondence should be addressed: paf3@georgetown.edu.

lesions(6). Disruption of p53 function may be involved in earlier rather than later stages of breast cancer progression such as initiation of breast carcinogenesis and impaired differentiation of DCIS (7,8). Alterations to p53 function include mutation, changes in upstream regulators, transcriptional target genes and coactivators (9). p53 detection in benign lesions, indicative of possible mutation, is associated with elevated cancer risk (10). In DCIS, p53 is associated with more advanced lesions (11) and is a predictor for local recurrence (12, 13). In cancers, loss or mutation of p53 is correlated with increased aggressiveness, poor prognosis (14) and chemotherapy resistance (15). In addition to p53 somatic mutation in sporadic cancers, germline mutation of one allele of this gene in humans causes an inborn predisposition to cancer known as Li-Fraumeni syndrome (16) where early-onset female breast cancer is the most prevalent tumor type (17).

Hormone receptor status is one of the main differentiating characteristics of human breast cancers and modifies therapeutic response. About 60-70% of human breast cancers are estrogen receptor  $\alpha$  (ER $\alpha$ ) positive and estrogen-dependent (18). Increased ER $\alpha$  expression in normal breast epithelium is found in conjunction with breast cancer, leading to the concept that loss of the normal regulatory mechanisms that control expression levels of ER $\alpha$  in normal breast epithelium may increase the risk for the development of breast cancer (19). Increased and deregulated ER $\alpha$  expression in the mammary epithelial cells of transgenic mice (CERM) results in the development of ductal carcinoma *in situ* and increased cell proliferation (20). Expression of ER $\alpha$  is increased two-fold in the mammary epithelial cells of these mice and is considered deregulated because it is not down-regulated by estrogen exposure.

Reproductive history is the strongest and most consistent risk factor outside of genetic background and age (21). Early pregnancy in reproductive life reduces breast cancer lifetime risk in women by up to 50% (22,23). In mouse models, p53 is required for hormonal protection from mammary tumorigenesis (24). Early exposure to estrogen and progesterone, designed to mimic pregnancy, has been found to enhance p53-dependent responses, increase resistance to carcinogenesis by blocking proliferation of ER $\alpha$ -positive cells (25), and suppress mammary tumor formation in BALB/c-Trp53<sup>+/-</sup> mice (26).

Different observations point to potential cross-talk between p53 and ER $\alpha$ . Human breast cancers with p53 mutations are more frequently ER-negative (27). In serial transplant studies, absence of p53 in mammary epithelium is associated with DCIS lesions and invasive cancer that progress from an ER $\alpha$ -positive to ER $\alpha$ -negative state (28,29). Studies have shown that p53 can regulate ER $\alpha$  expression and transcriptional activity but both positive and negative effects have been shown (30,31). ER $\alpha$  can also be regulated at the protein level. c-Src phosphorylation has been shown to stimulate ER $\alpha$  ubiquitylation and proteasome-dependent degradation (32) and p53 has been reported to down-regulate some Src functions (33).

The effects of loss of p53 and ER $\alpha$  deregulation on cell proliferation and apoptosis during *in vivo* carcinogenesis have been previously studied independently. Indeed, loss of p53 activity disrupts apoptosis and accelerates the appearance of tumors (34), and increases cell proliferation levels (35) while deregulated ER $\alpha$  increases cell proliferation and the prevalence of DH/DCIS (20). Studies in mouse models have shown that loss of p53 has a different impact in the susceptibility of mammary tumor development depending on the strain. C57BL/6 p53<sup>+/-</sup> mice are relatively resistant to mammary tumor development as compared to BALB/cJ (36).

The objective of this study was to utilize genetically engineered mouse models to investigate the impact of the combination of deregulated ER $\alpha$  and p53 haploinsufficiency and compare this to each factor alone in age-dependent mammary preneoplasia development, impact on cell proliferation and apoptosis, expression of regulatory proteins including ER $\alpha$ , and parity

protection. Each lesion independently and in combination increased age dependent development of mammary preneoplasia. Molecular studies revealed that only p53 heterozygosity impacted AKT activation and p27 expression while only the combination of deregulated ER $\alpha$  and p53 haploinsufficiency increased ERK1/2 and c-Src activation in association with decreased expression levels of ER $\alpha$ . Parity protected p53 heterozygous mice from developing mammary gland preneoplasia.

## Materials and Methods

### Mouse models, genotyping and necropsy

Mice carrying a transgene composed of the mouse mammary tumor virus-long terminal repeat (MMTV-LTR) linked to sequences encoding the tetracycline responsive reverse transactivator (rtTA) for “tet-on” gene regulation (37) and a transgene composed of the tetracycline operator (tet-op) promoter linked to sequences encoding murine ER $\alpha$  (38) [MMTV-rtTA/tet-op- ER $\alpha$  (CERM)] mice were bred to mice carrying a homozygous p53 mutation (Jackson Laboratory, Bar Harbor, ME) (39) to generate experimental CERM, p53<sup>+/-</sup> and compound CERM/p53<sup>+/-</sup> mice. Mice were maintained on a C57Bl/6 genetic background and nontransgenic wild-type (WT) littermates obtained from breedings were used as controls. All mice were maintained and euthanized in accordance with institutional and federal guidelines approved by the Georgetown University Animal Care and Use Committee and complete necropsies were performed at the specified euthanasia timepoints. MMTV-rtTA, tet-op- ER $\alpha$  transgenes and normal and disrupted p53 alleles were identified using tail samples (Transnetyx, Cordova, TN). Mice were maintained on a special diet containing 200 mg of doxycycline per kilogram food (Bio-Serv, French, NJ) during prenatal life until euthanized to induce transgene expression. Cohorts of nulliparous mice were euthanized at 4, 8 or 12 months of age to test the relationship between age and mammary preneoplasia development (4 and 8 month time-points, WT (n=10-12); p53<sup>+/-</sup> (n=10); CERM (n=10-13) and CERM/p53<sup>+/-</sup> (n=10); 12 month time-point, WT (n=25); p53<sup>+/-</sup> (n=25); CERM (n=25) and CERM/p53<sup>+/-</sup> (n=25). Mortality and morbidity was compared between female nulliparous mice (WT (n=59); p53<sup>+/-</sup> (n=64); CERM (n=63); and CERM/p53<sup>+/-</sup> (n=50)) but no statistically significant differences were found. Overall survival to age 12 months was 93% for WT, 84% for p53<sup>+/-</sup>, 90% for CERM, and 88% for CERM/p53<sup>+/-</sup>. Causes of premature death included euthanasia due to prolapsed anus (WT: n=1; p53<sup>+/-</sup>: n=1), skin infection (p53<sup>+/-</sup>: n=3; CERM: n=4), lymphoma (p53<sup>+/-</sup>: n=1), failure to thrive (WT: n=1; p53<sup>+/-</sup>: n=1; CERM: n=1; CERM/p53<sup>+/-</sup>: n=2), or found dead (WT: n=2; p53<sup>+/-</sup>: n=4; CERM: n=1; CERM/p53<sup>+/-</sup>: n=3). Cohorts of parous mice were mated at 2 months of age, underwent multiple pregnancies ( $\geq 3$ ), nursed their pups for 21 days, and were euthanized at  $\geq 10$  months of age to test the effects of parity on mammary preneoplasia development (WT (n=9; mean age 14.0 $\pm$ 1.0 months), p53<sup>+/-</sup> (n=7; mean age 13.2 $\pm$ 0.9 months); CERM (n=9; mean age 11.4 $\pm$ 0.7 months) and CERM/p53<sup>+/-</sup> (n=8; mean age 12.3 $\pm$ 0.5 months).

### Morphological and histological analyses of mammary glands

One inguinal mammary gland from each animal was dissected for whole mount preparation (40). Whole mounts were examined under 0.5x and 4x magnification to evaluate presence or absence of hyperplastic alveolar nodules (HANs). The other inguinal mammary gland was dissected and fixed in 10% buffered formalin overnight at 4°C and embedded in paraffin using standard techniques. Sections (5  $\mu$ m) were cut and stained with hematoxylin and eosin (H&E) staining and evaluated for the presence or absence of ductal hyperplasia (DH) and DCIS under a 60x magnification. DH/DCIS was defined as mammary ductal epithelium consisting of at least four epithelial cell layers that extended into and either partially or totally obliterated the lumen. Digital photographs were taken using a Nikon Eclipse E800M microscope with Nikon DMX1200 software (Nikon Instruments, Inc., Melville, NY).

## Immunohistochemistry (IHC)

Unstained 5  $\mu$ m tissue inguinal mammary gland sections were used for the detection of ER $\alpha$ , progesterone receptor (PgR), Src, and phospho (p)-Src using the Vectastain ABC kit (Vector Laboratories, Burlingame, CA). Detection of Ki67 was accomplished using the Mouse On Mouse (M.O.M) Peroxidase kit (Vector Laboratories, Inc., Burlingame, CA). *In situ* detection of apoptotic cell nuclei was performed using the ApopTag® Plus Peroxidase *In Situ* Apoptosis Kit (Millipore, Billerica, MA). Sections were deparaffinized, rehydrated, and boiled for 20 minutes in citrate buffer, pH 6.0 for antigen retrieval and endogenous peroxidase activity was inactivated by 10 minutes incubation in 3% hydrogen peroxide at room temperature. Tissues were blocked with the appropriate IgG-blocking reagent (10m), exposed to the appropriate primary antibody (1h) and to biotinylated anti-rabbit or anti-mouse IgG secondary antibody (30m), exposed to ABC reagent for (30m), stained with DAB chromogen (Dako, Carpinteria, CA) (5m) and counterstained with hematoxylin. Primary antibodies included: 1:500 dilution of rabbit polyclonal ER $\alpha$  antibody sc-542 (Santa Cruz Biotechnology, Inc., Santa Cruz, CA); 1:250 dilution of rabbit polyclonal Progesterone Receptor (PgR) antibody sc-538 (Santa Cruz Biotechnology); 1:800 dilution of rabbit monoclonal Src (36D10) antibody (Cell Signaling Technology, Danvers, MA); 1:25 dilution of rabbit polyclonal p-Src (Tyr 416) antibody (Cell Signaling Technology); 1:100 dilution of mouse monoclonal Ki-67 antibody RTU-Ki67-MM1 (Novocastra, UK). Proliferative Index (PI) and Apoptotic Index (AI) were calculated as percentage of mammary epithelial cells demonstrating stained nuclei in the total of at least 1000 cells per section. The percentage of mammary epithelial cells demonstrating nuclear-localized ER $\alpha$  and PgR were calculated by counting 1000 cells per mouse. p-Src IHC was scored using a combination of the percentage of mammary epithelial cells demonstrating staining and stain intensity as read by two independent observers: 1=<33% cells stained at low intensity; 2=between 33 and 66% of cells stained at low intensity; 3=>66% of cells stained at low intensity; 4=>66% of cells stained at high intensity. Five sections were randomly selected from each experimental and control group for staining. Negative control slides in which primary antibody was omitted, were analyzed in parallel. In the absence of primary antibody no nuclear-specific staining was observed for ER $\alpha$ , PgR and Ki67 and no cell specific staining for p-Src and Src.

## Immunoblotting

Dissected thoracic mammary gland was homogenized in RIPA buffer (Cell Signaling Technology) containing 1mM PMSF plus protease and phosphatase inhibitors (Roche Diagnostics, Indianapolis, IN). After plunging the lysates with a syringe needle followed by centrifugation, supernatant protein concentration was measured using the BCA Protein Assay Kit (Pierce, Rockford, IL). Protein samples (60 $\mu$ g per sample) were resolved by using 4-12% gradient SDS-PAGE (Invitrogen, Carlsbad, CA), transferred onto nitrocellulose membranes (Hybond ECL, GE Healthcare Bio-sciences, Piscataway, NJ). Unless noted otherwise, all primary antibodies were from Cell Signaling Technology and used at a concentration of 1:1,000. Primary antibodies included phospho-p44/42 MAPK (E10), p44/42 MAPK, phospho-Akt (D9E), Akt (C67E7), and p27 Kip1. p53 (FL-393) and actin (I-19) were obtained from Santa Cruz Biotechnology. Secondary antibodies included rabbit anti-goat sc-2768 and anti-mouse sc-2005 (Santa Cruz Biotechnology) and anti-rabbit (GE Healthcare Bio-Sciences). Four independent samples were randomly selected from each experimental and control group for western blot analysis.

## RNA isolation and gene expression analysis by semi-quantitative RT-PCR

Total RNA was isolated by using TRIzol reagent (Invitrogen) from thoracic mammary gland tissue snap frozen at the time of necropsy, quantified on a spectrophotometer, and 2 $\mu$ g of total RNA were used to prepare cDNA by a reverse-transcriptase (RT) reaction. Semi-quantitative

RT-Polymerase Chain Reaction (PCR) was performed by using REDTaq® DNA polymerase (Sigma-Aldrich, St. Louis, MO). Cycle numbers were tested for each primer combination to determine the cycle number when the reaction became saturated. The following primers were used for amplification; tet-op-ER $\alpha$ : forward, CCACACCAGCCACCACCTTC; reverse, CCACTTCAGCACATTCCTTA; ER $\alpha$ : forward, GACCAGATGGTCAGTGCCTT; reverse, GACCAGATGGTCAGTGCCTT; PgR b: forward, GGTCCCCCTTGCTTGCA; reverse, CAGGACCGAGGAAAAAGCAG; PgR a+b: forward, GGTGGGCCTTCCTAACGAG; reverse, GACCACATCAGGCTCAATGCT; p53: forward, GGGACAGCCAAGTCTGTTATG; reverse, GGAGTCTTCCAGTGTGATGAT; actin: forward, ATCGTGGGCCGCCCTAGGCA; reverse, TGGCCTTAGGGTTCAGAGGG. PCR gels were visualized by using the UV transilluminator FBTI-816 (Fisher Scientific, Pittsburgh, PA), images captured using Kodak EDAS 290 (Kodak, Rochester, NY) and analyzed using Kodak 1D LE 3.6 and Scion Image (Scion Corporation, Bethesda, MD) software. Four independent samples were randomly selected from each experimental and control group for RNA analysis.

### Statistical analyses

Statistical differences among groups were analyzed with Fisher's exact for HAN and DH/DCIS prevalence, *t* test for ER $\alpha$ , PgR, Ki67, ApopTag levels, and Mann-Whitney for p-Src scoring using GraphPad Prism version 4.03 for Windows (GraphPad Software, San Diego, CA). Mean data is presented as mean  $\pm$  Standard Error of the Mean (SEM). Significance was assigned at  $P \leq 0.05$ .

## Results

### p53 deficiency and deregulated ER $\alpha$ expression collaborated to increase prevalence of age dependent mammary preneoplasia

To test the relationship between age and mammary preneoplasia development secondary to p53 deficiency and/or deregulated ER $\alpha$  expression, HAN (Fig. 1A) and DH/DCIS (Fig. 1B) prevalence was compared in mammary glands from nulliparous mice aged 4, 8 and 12 months. At 4 months of age none of the mice had developed HANs but by 8 months of age at least 20% of the mice from all three experimental genotypes demonstrated HANs (Fig. 1C). By 12 months of age HAN prevalence was significantly increased in CERM/p53<sup>+/-</sup> mice as compared to the 4 and 8-month timepoints (71% vs. 0%,  $P \leq 0.0001$ ; and 71% vs. 20%,  $P \leq 0.008$ , respectively). By 12 months of age HAN prevalence was significantly increased in p53<sup>+/-</sup> as compared to the 4-month timepoint (35% vs. 0%,  $P = 0.04$ ); with a more modest increase as compared to the 8-month timepoint (35% vs. 20%). By 12 months of age HAN prevalence increased to 32% in CERM mice as compared to 30% at 8 months and 0% at 4 months. No WT mice demonstrated HANs at either 4 or 8 months but by 12 months of age, HAN prevalence increased to 8%. DH/DCIS appeared earlier and at 4 months of age was found in all three experimental groups CERM/p53<sup>+/-</sup> (50%), CERM (23%), p53<sup>+/-</sup> (40%) but not in WT mice (Fig. 1C). Prevalence rates remained approximately the same at 8 months of age in all genotypes. Like HAN prevalence, by 12 months of age DH/DCIS prevalence was increased in CERM/p53<sup>+/-</sup> mice as compared to 8 months of age (60% vs. 40%). WT mice demonstrated a 4% DH/DCIS prevalence rate at 12 months of age. In summary, while all mice showed an increase in HAN and DH/DCIS prevalence with age, the combination of deregulated ER $\alpha$  and p53 deficiency demonstrated the highest prevalence and most significant increases in age-related preneoplasia development as compared to either deregulated ER $\alpha$  or p53 deficiency alone.

### **p53 deficiency and deregulated ER $\alpha$ expression collaborated to increase rates of cell proliferation and reduce rates of apoptosis**

To test if changes in the rates of either cell proliferation or apoptotic cell death were correlated with the higher prevalence of preneoplasia in the CERM/p53<sup>+/-</sup> mice, proliferative (PI) and apoptotic (AI) indexes were compared between genotypes at 12 months of age (Fig. 2, A-C). The combination of deregulated ER $\alpha$  and p53 deficiency showed the highest PI (41 $\pm$ 1%) as compared to 24 $\pm$ 1%, 23 $\pm$ 3% and 0.4 $\pm$ 0.3, respectively, in CERM, p53<sup>+/-</sup> and WT mice (all  $P\leq 0.0004$ ). The AI was lowest in CERM/p53<sup>+/-</sup> (0.06 $\pm$ 0.04%) mice but all three experimental genotypes (CERM: 0.19 $\pm$ 0.08%; p53<sup>+/-</sup>: 0.12 $\pm$ 0.06%) were significantly lower than WT mice (0.66 $\pm$ 0.06%) (all  $P\leq 0.0009$ ). In summary, while all three experimental genotypes demonstrated abnormal apoptotic and proliferation rates, the mice with both deregulated ER $\alpha$  and p53 deficiency demonstrated the most abnormal parameters.

### **Protein expression changes associated with p53 deficiency and deregulated ER $\alpha$ expression**

Experiments were performed to test if changes in proliferation or apoptosis related genes were associated with the altered proliferation and apoptotic rates. At 12 months of age, all three experimental genotypes demonstrated increased levels of ERK1/2 activation, however only mice with p53 heterozygosity (CERM/p53<sup>+/-</sup> and p53<sup>+/-</sup>) showed increased AKT activation and decreased p27 expression (Fig. 2D). Experiments were also performed to compare levels of p53, ER $\alpha$  and PgR, as an ER $\alpha$  downstream gene target, in the experimental and WT mice. Reduced levels of p53 expression at both protein and RNA levels were confirmed in p53 heterozygous mice (Fig. 2D, and 3C). The mean percentage of mammary epithelial cells demonstrating nuclear-localized ER $\alpha$  was significantly increased in CERM (18.30 $\pm$ 0.08%) as compared to p53<sup>+/-</sup> (8.8 $\pm$ 0.2%), and wild-type mice (8.3 $\pm$ 0.9%), (both  $P\leq 0.0001$ ) (Fig. 3A,B). While the mean percentage of nuclear-localized ER $\alpha$  was significantly decreased in CERM/p53<sup>+/-</sup> (6.9 $\pm$ 0.3%), as compared to CERM mice ( $P\leq 0.0001$ ), nuclear-localized PgR was increased in both CERM/p53<sup>+/-</sup> (16.5 $\pm$ 1.8%) and CERM (13.9 $\pm$ 0.4%) as compared to p53<sup>+/-</sup> (9.1 $\pm$ 0.1%) and control (9.7 $\pm$ 1.0%) mice (all  $P\leq 0.02$ ) (Fig. 3A,B). The DH/DCIS lesions observed in CERM/p53<sup>+/-</sup> stained positive for nuclear-localized ER $\alpha$ . To evaluate if the decrease in nuclear-localized ER $\alpha$  expression occurred at the protein level in the CERM/p53<sup>+/-</sup> mice or was associated with decreased RNA levels, RNA from mammary gland tissues was analyzed using semi-quantitative RT-PCR. Equivalent levels of transgene specific ER $\alpha$  were found in CERM and CERM/p53<sup>+/-</sup> mice and levels of ER $\alpha$ , total PgR and isoform b PgR RNA were not significantly different between genotypes (Fig. 3C). To determine if the decrease in ER $\alpha$  protein in the compound mice was associated with higher p-Src levels, relative levels of p-Src and Src were scored in the different genotypes. p-Src scores were significantly higher in CERM/p53<sup>+/-</sup> (3.8 $\pm$ 0.3) as compared to CERM (1.8 $\pm$ 0.3), p53<sup>+/-</sup> (1.8 $\pm$ 0.5), and WT (1.3 $\pm$ 0.3) mice (Fig. 3A) ( $p\leq 0.05$ ). In summary, the changes in proliferation and apoptotic rates were accompanied by expression changes in apoptosis and proliferation-related proteins with changes in p53, phospho-AKT and p27 associated with p53 heterozygosity. Decreased expression levels of ER $\alpha$  in CERM/p53<sup>+/-</sup> mice were associated with increased levels of p-Src expression.

### **Parity protected p53 deficient mice from developing mammary preneoplasia with attenuation by deregulated ER $\alpha$ expression**

To test if parity impacted disease progression, cohorts of CERM/p53<sup>+/-</sup>, CERM, p53<sup>+/-</sup> and WT mice were continuously mated beginning at 2 months of age and HAN and DH/DCIS prevalence compared after serial pregnancies (Fig. 4). Parous p53<sup>+/-</sup> mice showed a significant absence of HAN development following serial pregnancy that was not seen in CERM mice ( $P<0.03$ ) or other genotype. DH/DCIS prevalence showed a similar trend with the CERM/p53<sup>+/-</sup> mice demonstrating no DH/DCIS compared to a 60% prevalence in nulliparous mice

( $P < 0.004$ ). Parity did not alter the mean percentage of mammary epithelial cells demonstrating nuclear-localized ER $\alpha$ . Like nulliparous mice, ER $\alpha$  expression was significantly increased in parous CERM (13.1 $\pm$ 0.6%) as compared to CERM/p53 $^{+/-}$  (6.0 $\pm$ 0.6%), p53 $^{+/-}$  (6.1 $\pm$ 0.6%) and WT (6.7 $\pm$ 0.2%) mice, (all  $P \leq 0.0002$ ) (Fig. 4C). In summary, parity was associated with a reduction in preneoplasia only in cohorts where p53 haploinsufficiency played a role.

## Discussion

This *in vivo* study demonstrated that deregulated ER $\alpha$  and p53 have independent and collaborating roles in the genesis of mammary preneoplasia. While both deregulated estrogen signaling pathways and loss of p53 function have been previously implicated in breast cancer development, this study demonstrated that the two lesions have additive effects in promoting abnormal mammary epithelial cell growth. Instructive aspects of the study were the focus on p53 heterozygosity as compared to complete loss of p53, comparison of two types of proliferative lesions (DH/DCIS and HANs), and investigation of the impact of both age and parity on prevalence of preneoplasia. The fact that a decrease but not complete loss of p53 was sufficient to induce the development of preneoplasia is compatible with the increased risk of breast cancer found in women with Li-Fraumeni syndrome (16,17). The fact that the prevalence of preneoplasia increased with age is consistent with the increased incidence of breast cancer with age in women (1) and suggests that duration of a molecular lesion and/or cellular changes associated with aging are additional risk factors for preneoplasia development.

Breast epithelial cell homeostasis requires the balance of cell proliferation and apoptosis (41). In this study both deregulated ER $\alpha$  and p53 heterozygosity independently and in combination altered this balance. The changes were associated with increased activation of ERK1/2. Changes in AKT activation were limited to either the p53 heterozygous mice or the combination. *In vitro*, estrogen signaling has been associated with activation of both ERK1/2 and AKT (42). These results indicate that *in vivo* loss of p53 function is more potent than deregulated ER $\alpha$  in inducing AKT activation. Activation of ERK1/2 and AKT are frequently found in different types of transformed cells and may influence chemotherapeutic drug resistance (43).

The cell cycle inhibitor p27 has been referred to as a candidate tumor suppressor (44) and the presence of functional p53 correlates with p27 expression in human breast cancer (45). p27 expression has been documented in human DCIS, but its clinicopathological significance remains unclear (46). Reduced p27 levels due to protein degradation occurs in half of carcinomas (including breast) and correlates with aggressive, high-grade tumors and poor prognosis (47). Low nuclear p27 levels are correlated with c-Src activation in human breast cancers and *in vitro* studies have shown that c-Src activation increases p27 phosphorylation mediating p27 proteolysis and driving cell proliferation (48). Our results showed decreased levels of p27 protein in the p53 deficient mice.

In the normal pre-menopausal breast, ER $\alpha$ -positive cells comprise 7% of the total epithelial cell population (49) similar to what we observed in wild-type mice here (8.3%). As reported previously, the mice with deregulated ER $\alpha$  in this study showed an approximately two-fold increase in mammary epithelial cells with nuclear localized ER $\alpha$  (20). However, the CERM/p53 $^{+/-}$  mice showed a significant decrease in the percentage of mammary epithelial cells with nuclear-localized ER $\alpha$  independent from any detectable changes in RNA expression. Both transcriptional and post-transcriptional mechanisms regulate ER $\alpha$  protein expression levels. Studies demonstrate that c-Src cooperates with estrogen to activate ER $\alpha$  proteolysis, and that increased c-Src activation leads to a reduced ER $\alpha$  half-life and increased ER $\alpha$ -driven transcription (32). The highest levels of the activated p-Src (Tyr416) were found with the combination of deregulated ER $\alpha$  and p53 deficiency while expression of the ER $\alpha$  down stream

gene PgR was maintained. It is possible that p-Src plays a role in the observed reduction in ER $\alpha$  protein expression in this genotype. Mdm2 and p53 also have been implicated in the regulation of ER $\alpha$  protein degradation (50). Mdm2 over expression in the absence of p53 can promote estrogen ligand independent degradation of ER $\alpha$ . It is also possible that the reduction of p53 expression increased availability of Mdm2 leading to increased turnover of ER $\alpha$ .

Studies have shown that pregnancy early in reproductive life confers a 50% reduction in lifetime breast cancer risk (22), and that parity is protective in the BALB/c-*Trp53*<sup>+/-</sup> mice (26). We evaluated the effect of pregnancy on the development of mammary gland preneoplasia in four genotypes of mice on a C57Bl/6 background. A noticeable decrease in preneoplasia in p53 deficient mice but not in mice with deregulated ER $\alpha$  alone or WT mice was found, suggesting a possible protective effect of pregnancy in mice with disease initiated by loss of p53 function. This protection may be due to increased activation of p53 signaling through pregnancy (25) that compensated for its reduced expression levels.

As our knowledge of molecular biomarkers increases, risk assessment may include possible “interacting biomarkers” along with specific clinical, genetic, environmental and pathological factors. Our data demonstrated that deregulation of ER $\alpha$  in the mammary gland and reduced p53 expression are independent but additive genetic determinants of increased risk that can be impacted by both age and parity and suggest these factors could function together as an “interacting biomarker”. These mouse models could be used to test possible preventive strategies that could mimic protective hormonal changes that occur during pregnancy with follow-up at the molecular level to identify critical signaling events that might serve as markers of response in women. The fact that preneoplasia was not prevented by parity in either the mice with deregulated ER $\alpha$  alone or the WT mice suggests that not all risk factors associated with increased breast cancer risk can be reduced by pregnancy. This is consistent with the appearance of human breast cancer in both parous and non-parous women.

## Acknowledgments

These studies were conducted in part using the Lombardi Comprehensive Cancer Center Histopathology and Tissue Shared Resource, and the Animal Shared Resource Core Facilities. We thank Massod Rahimi for scientific discussions and technical assistance.

**Financial support:** This work was supported by grant NCI, NIH 1R01CA112176 (P.A. Furth); NCI, “Research Supplements to Promote Diversity in Health-Related Research,” (E.S. Díaz-Cruz) and Susan G. Komen for the Cure Postdoctoral Fellowship, KG080359 (E.S. Díaz-Cruz).

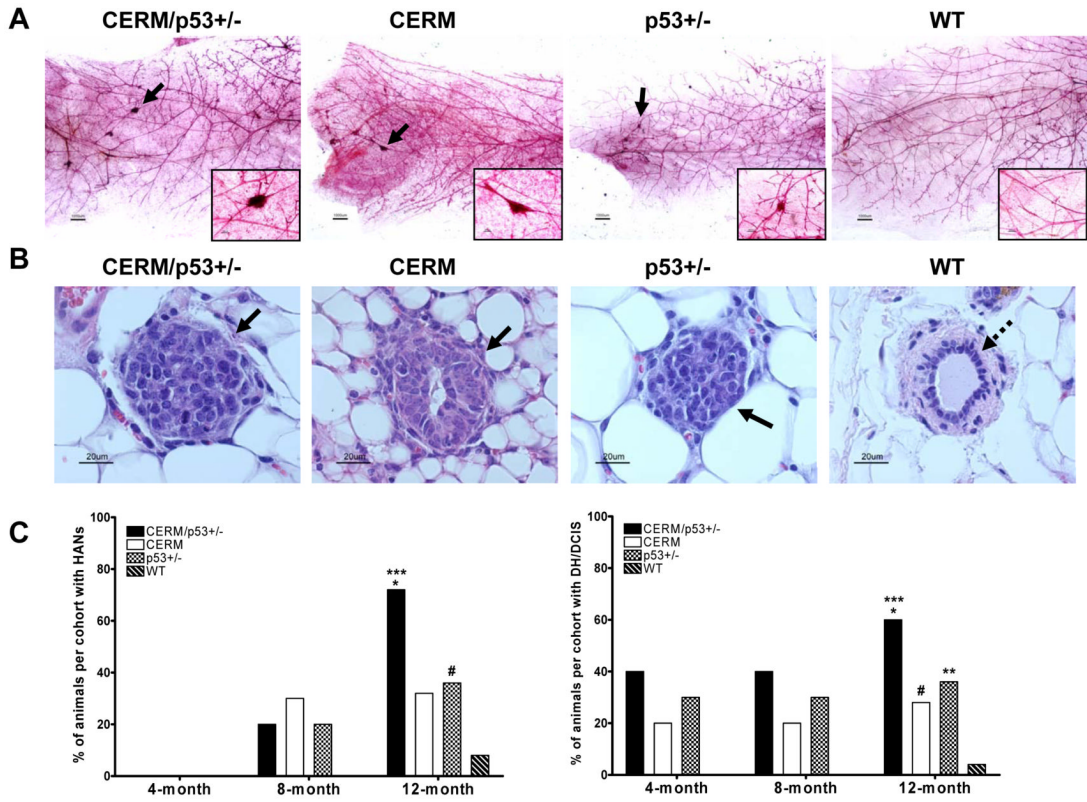
## References

1. Glass AG, Lacey JV Jr, Carreon JD, Hoover RN. Breast cancer incidence, 1980-2006: combined roles of menopausal hormone therapy, screening mammography, and estrogen receptor status. *J Natl Cancer Inst* 2007;99:1152–61. [PubMed: 17652280]
2. Lakhani SR. The transition from hyperplasia to invasive carcinoma of the breast. *J Pathol* 1999;187:272–8. [PubMed: 10398078]
3. Lacroix M, Toillon RA, Leclercq G. p53 and breast cancer, an update. *Endocr Relat Cancer* 2006;13:293–325. [PubMed: 16728565]
4. Varley JM, Brammar WJ, Lane DP, Swallow JE, Dolan C, Walker RA. Loss of chromosome 17p13 sequences and mutation of p53 in human breast carcinomas. *Oncogene* 1991;6:413–21. [PubMed: 2011397]
5. Elledge RM, Allred DC. The p53 tumor suppressor gene in breast cancer. *Breast Cancer Res Treat* 1994;32:39–47. [PubMed: 7819584]
6. Rudas M, Neumayer R, Gnant MF, Mittelbock M, Jakesz R, Reiner A. p53 protein expression, cell proliferation and steroid hormone receptors in ductal and lobular in situ carcinomas of the breast. *Eur J Cancer* 1997;33:39–44. [PubMed: 9071897]

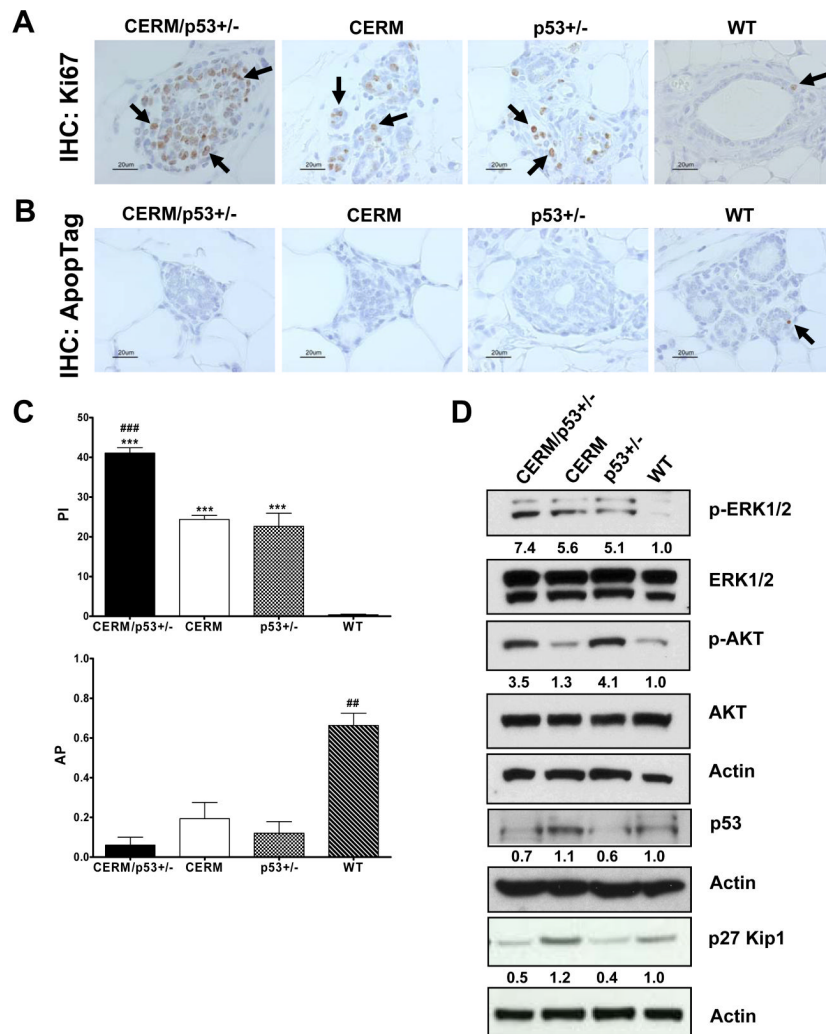


7. Mommers EC, Leonhart AM, Falix F, et al. Similarity in expression of cell cycle proteins between in situ and invasive ductal breast lesions of same differentiation grade. *J Pathol* 2001;194:327–33. [PubMed: 11439365]
8. Warnberg F, Nordgren H, Bergkvist L, Holmberg L. Tumour markers in breast carcinoma correlate with grade rather than with invasiveness. *Br J Cancer* 2001;85:869–74. [PubMed: 11556839]
9. Gasco M, Shami S, Crook T. The p53 pathway in breast cancer. *Breast Cancer Res* 2002;4:70–6. [PubMed: 11879567]
10. Rohan TE, Hartwick W, Miller AB, Kandel RA. Immunohistochemical detection of c-erbB-2 and p53 in benign breast disease and breast cancer risk. *J Natl Cancer Inst* 1998;90:1262–9. [PubMed: 9731732]
11. Mack L, Kerkvliet N, Doig G, O'Malley FP. Relationship of a new histological categorization of ductal carcinoma in situ of the breast with size and the immunohistochemical expression of p53, c-erb B2, bcl-2, and ki-67. *Hum Pathol* 1997;28:974–9. [PubMed: 9269835]
12. Hieken TJ, Cheregi J, Farolan M, Kim J, Velasco JM. Predicting relapse in ductal carcinoma in situ patients: an analysis of biologic markers with long-term follow-up. *Am J Surg* 2007;194:504–6. [PubMed: 17826066]
13. de Roos MA, de Bock GH, de Vries J, van der Vegt B, Wesseling J. p53 overexpression is a predictor of local recurrence after treatment for both in situ and invasive ductal carcinoma of the breast. *J Surg Res* 2007;140:109–14. [PubMed: 17291532]
14. Greenblatt MS, Bennett WP, Hollstein M, Harris CC. Mutations in the p53 tumor suppressor gene: clues to cancer etiology and molecular pathogenesis. *Cancer Res* 1994;54:4855–78. [PubMed: 8069852]
15. Lowe SW, Bodis S, McClatchey A, et al. p53 status and the efficacy of cancer therapy in vivo. *Science* 1994;266:807–10. [PubMed: 7973635]
16. Malkin D, Li FP, Strong LC, et al. Germ line p53 mutations in a familial syndrome of breast cancer, sarcomas, and other neoplasms. *Science* 1990;250:1233–8. [PubMed: 1978757]
17. Varley JM, Evans DG, Birch JM. Li-Fraumeni syndrome--a molecular and clinical review. *Br J Cancer* 1997;76:1–14. [PubMed: 9218725]
18. Li CI, Daling JR, Malone KE. Incidence of invasive breast cancer by hormone receptor status from 1992 to 1998. *J Clin Oncol* 2003;21:28–34. [PubMed: 12506166]
19. Khan SA, Rogers MA, Khurana KK, Meguid MM, Numann PJ. Estrogen receptor expression in benign breast epithelium and breast cancer risk. *J Natl Cancer Inst* 1998;90:37–42. [PubMed: 9428781]
20. Frech MS, Halama ED, Tilli MT, et al. Deregulated estrogen receptor alpha expression in mammary epithelial cells of transgenic mice results in the development of ductal carcinoma in situ. *Cancer Res* 2005;65:681–5. [PubMed: 15705859]
21. Kelsey JL, Gammon MD. The epidemiology of breast cancer. *CA Cancer J Clin* 1991;41:146–65. [PubMed: 1902137]
22. Bernstein L. Epidemiology of endocrine-related risk factors for breast cancer. *J Mammary Gland Biol Neoplasia* 2002;7:3–15. [PubMed: 12160084]
23. Harris JR, Lippman ME, Veronesi U, Willett W. Breast cancer (1). *N Engl J Med* 1992;327:319–28. [PubMed: 1620171]
24. Medina D, Kittrell FS. p53 function is required for hormone-mediated protection of mouse mammary tumorigenesis. *Cancer Res* 2003;63:6140–3. [PubMed: 14559792]
25. Sivaraman L, Conneely OM, Medina D, O'Malley B. p53 is a potential mediator of pregnancy and hormone-induced resistance to mammary carcinogenesis. *Proc Natl Acad Sci U S A* 2001;98:12379–84. [PubMed: 11606748]
26. Dunphy KA, Blackburn AC, Yan H, O'Connell LR, Jerry DJ. Estrogen and progesterone induce persistent increases in p53-dependent apoptosis and suppress mammary tumors in BALB/c-Trp53+/- mice. *Breast Cancer Res* 2008;10:R43. [PubMed: 18471300]
27. Putti TC, El-Rehim DM, Rakha EA, et al. Estrogen receptor-negative breast carcinomas: a review of morphology and immunophenotypical analysis. *Mod Pathol* 2005;18:26–35. [PubMed: 15332092]
28. Medina D, Kittrell FS, Shepard A, et al. Biological and genetic properties of the p53 null preneoplastic mammary epithelium. *Faseb J* 2002;16:881–3. [PubMed: 11967232]

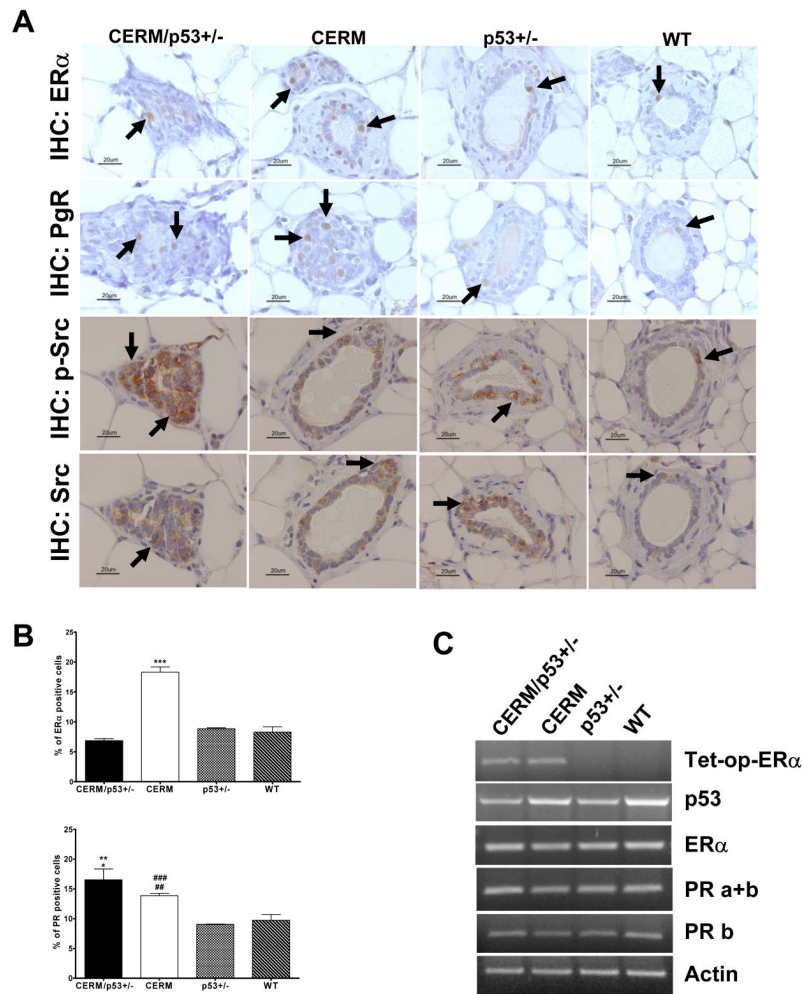
29. Medina D, Kittrell FS, Shepard A, Contreras A, Rosen JM, Lydon J. Hormone dependence in premalignant mammary progression. *Cancer Res* 2003;63:1067–72. [PubMed: 12615724]
30. Akaogi K, Nakajima Y, Ito I, et al. KLF4 suppresses estrogen-dependent breast cancer growth by inhibiting the transcriptional activity of ERalpha. *Oncogene* 2009;28:2894–902. [PubMed: 19503094]
31. Shirley SH, Rundhaug JE, Tian J, et al. Transcriptional regulation of estrogen receptor-alpha by p53 in human breast cancer cells. *Cancer Res* 2009;69:3405–14. [PubMed: 19351845]
32. Chu I, Arnaout A, Loiseau S, et al. Src promotes estrogen-dependent estrogen receptor alpha proteolysis in human breast cancer. *J Clin Invest* 2007;117:2205–15. [PubMed: 17627304]
33. Mukhopadhyay UK, Eves R, Jia L, Mooney P, Mak AS. p53 suppresses Src-induced podosome and rosette formation and cellular invasiveness through the upregulation of caldesmon. *Mol Cell Biol* 2009;29:3088–98. [PubMed: 19349302]
34. Attardi LD, Jacks T. The role of p53 in tumour suppression: lessons from mouse models. *Cell Mol Life Sci* 1999;55:48–63. [PubMed: 10065151]
35. Jones JM, Attardi L, Godley LA, et al. Absence of p53 in a mouse mammary tumor model promotes tumor cell proliferation without affecting apoptosis. *Cell Growth Differ* 1997;8:829–38. [PubMed: 9269892]
36. Koch JG, Gu X, Han Y, et al. Mammary tumor modifiers in BALB/cJ mice heterozygous for p53. *Mamm Genome* 2007;18:300–9. [PubMed: 17557176]
37. Gunther EJ, Belka GK, Wertheim GB, et al. A novel doxycycline-inducible system for the transgenic analysis of mammary gland biology. *Faseb J* 2002;16:283–92. [PubMed: 11874978]
38. Hruska KS, Tilli MT, Ren S, et al. Conditional over-expression of estrogen receptor alpha in a transgenic mouse model. *Transgenic Res* 2002;11:361–72. [PubMed: 12212839]
39. Jacks T, Remington L, Williams BO, et al. Tumor spectrum analysis in p53-mutant mice. *Curr Biol* 1994;4:1–7. [PubMed: 7922305]
40. Tilli MT, Frech MS, Steed ME, et al. Introduction of estrogen receptor-alpha into the tTA/TAg conditional mouse model precipitates the development of estrogen-responsive mammary adenocarcinoma. *Am J Pathol* 2003;163:1713–9. [PubMed: 14578170]
41. Alenzi FQ. Links between apoptosis, proliferation and the cell cycle. *Br J Biomed Sci* 2004;61:99–102. [PubMed: 15250676]
42. Fox EM, Andrade J, Shupnik MA. Novel actions of estrogen to promote proliferation: integration of cytoplasmic and nuclear pathways. *Steroids* 2009;74:622–7. [PubMed: 18996136]
43. McCubrey JA, Steelman LS, Chappell WH, et al. Roles of the Raf/MEK/ERK pathway in cell growth, malignant transformation and drug resistance. *Biochim Biophys Acta* 2007;1773:1263–84. [PubMed: 17126425]
44. Vervoorts J, Luscher B. Post-translational regulation of the tumor suppressor p27(KIP1). *Cell Mol Life Sci* 2008;65:3255–64. [PubMed: 18636226]
45. Casalini P, Iorio MV, Berno V, et al. Relationship between p53 and p27 expression following HER2 signaling. *Breast* 2007;16:597–605. [PubMed: 17604627]
46. Oh YL, Choi JS, Song SY, et al. Expression of p21Waf1, p27Kip1 and cyclin D1 proteins in breast ductal carcinoma in situ: Relation with clinicopathologic characteristics and with p53 expression and estrogen receptor status. *Pathol Int* 2001;51:94–9. [PubMed: 11169147]
47. Slingerland J, Pagano M. Regulation of the cdk inhibitor p27 and its deregulation in cancer. *J Cell Physiol* 2000;183:10–7. [PubMed: 10699961]
48. Chu I, Sun J, Arnaout A, et al. p27 phosphorylation by Src regulates inhibition of cyclin E-Cdk2 and p27 proteolysis. *Cell* 2007;128:281–94. [PubMed: 17254967]
49. Petersen OW, Hoyer PE, van Deurs B. Frequency and distribution of estrogen receptor-positive cells in normal, nonlactating human breast tissue. *Cancer Res* 1987;47:5748–51. [PubMed: 3664479]
50. Duong V, Boulle N, Daujat S, et al. Differential regulation of estrogen receptor alpha turnover and transactivation by Mdm2 and stress-inducing agents. *Cancer Res* 2007;67:5513–21. [PubMed: 17545634]



**Figure 1.** p53 deficiency and deregulated ER $\alpha$  expression in mammary epithelial cells led to the development of preneoplastic mammary gland lesions in nulliparous mice. *A*, representative mammary gland whole mounts (reference bar = 1000 $\mu$ m) from mice at age 12 months. *Black arrows* and magnified region indicate the presence of HANs. *B*, representative mammary glands tissue sections stained with H&E showing DH/DCIS (*black arrows*); and normal duct development (*dashed arrows*) in mice at age 12 months. *C, left*, HAN prevalence per genotype at age 4, 8 and 12 months. *\*\*\**,  $P \leq 0.0001$  vs. WT, *\**,  $P \leq 0.05$  vs. CERM and p53 $^{+/-}$ , *#*,  $P \leq 0.05$  vs. WT. *Right*, DH/DCIS prevalence per genotype at age 4, 8 and 12 months. *\*\*\**,  $P \leq 0.0001$  vs. WT; *\**,  $P \leq 0.05$  vs. CERM; *#*,  $P \leq 0.05$  vs. WT; and *\*\**,  $P \leq 0.05$  vs. WT. Data are expressed as percent of animals with HANs or DH/DCIS per genotype, and analyzed using Fisher's Exact test.



**Figure 2.** Deregulation of ER $\alpha$  expression in the mammary epithelial cells of p53 deficient nulliparous mice resulted in higher rates of cell proliferation and reduced rates of apoptosis in the mammary gland at 12 months of age. *A*, representative immunohistochemical (IHC) detection of the cell proliferation marker Ki67. *B*, representative IHC detection of ApopTag staining. *Black arrows* indicate the presence of cells demonstrating nuclear-localized protein. *C*, quantification of Ki67 positive cells (*top*), and ApopTag positive cells (*bottom*). Columns, mean of five independent experiments; bars, SEM. \*\*\*,  $P \leq 0.0001$  vs WT; ###,  $P \leq 0.0005$  vs CERM and p53<sup>+/-</sup>; ##,  $P \leq 0.001$  vs CERM/p53<sup>+/-</sup>, CERM and p53<sup>+/-</sup>, by unpaired one-tailed t-test. *D*, Western blot analysis of whole cell protein extracts from mammary gland tissues for cell proliferation protein markers and total actin. Band intensity was quantified and normalized based on total protein loaded against WT mice.

**Figure 3.**

Differential expression of ER $\alpha$ , PgR and p-Src in the mammary gland. *A*, representative IHC detection of nuclear expression of ER $\alpha$ , PgR nuclear staining, p-Src (Tyr416), and Src. *Black arrows* indicate the presence of cells demonstrating nuclear-localized protein. *B*, quantification of ER $\alpha$  positive cells (*top*) and PgR positive cells (*bottom*) in the mammary gland. \*\*\*,  $P \leq 0.0002$  vs CERM/p53<sup>+/-</sup>, p53<sup>+/-</sup> and WT; \*\*,  $P \leq 0.008$  vs p53<sup>+/-</sup>; \*,  $P \leq 0.02$  vs WT; ###,  $P \leq 0.0002$  vs p53<sup>+/-</sup>; ##,  $P \leq 0.009$  vs WT, by unpaired one-tailed t-test. *C*, representative semi-quantitative RT-PCR analysis of extracted RNA from mammary gland tissues for tet-op-ER $\alpha$ , p53, ER $\alpha$ , PgR a+b, PgR b and actin.

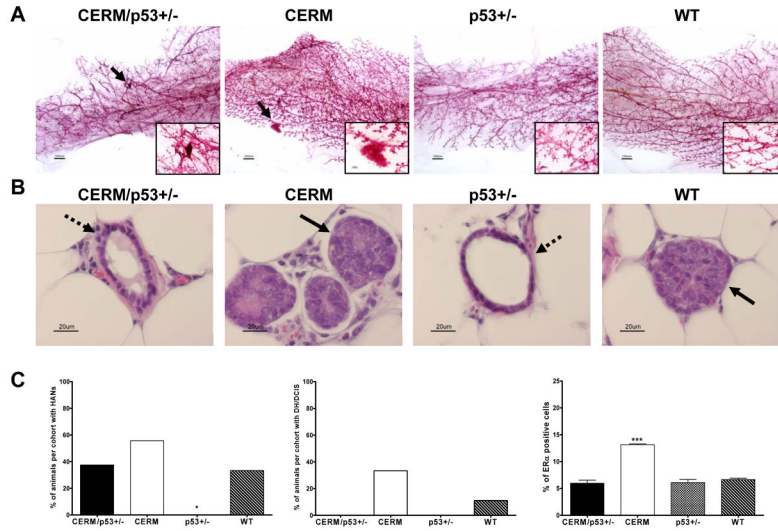


**Figure 4.** Pregnancy protected p53 deficient mice from developing mammary gland preneoplasia. *A*, representative mammary gland whole mounts (reference bar = 1000μM) from parous mice. *Black arrows* and magnified region indicate the presence of HANs. *B*, representative mammary glands tissue sections stained with H&E showing signs of DCIS (*black arrows*) and normal ductal development (*dashed arrows*). *C*, *left*, HAN prevalence per genotype in multi-parous mice. *Middle*, DH/DCIS prevalence per genotype in multiparous mice. *Right*, quantification of ERα positive cells in the mammary gland. Data are expressed as percent of animals with HANs, DH/DCIS or ERα staining per genotype, and analyzed using Fisher’s exact test or by unpaired one-tailed *t*-test. \*,  $P \leq 0.05$  vs. CERM; \*\*\*,  $P \leq 0.0001$  vs. CERM/p53<sup>+/-</sup>, p53<sup>+/-</sup> and WT.